

Pressure-induced cubic-to-orthorhombic phase transformation in the negative thermal expansion material HfW_2O_8

J. D. Jorgensen,^{a)} Z. Hu, and S. Short

Materials Science Division, Argonne National Laboratory, Argonne, Illinois 60439

A. W. Sleight

Department of Chemistry and Center for Advanced Materials Research, Oregon State University, Corvallis, Oregon 97331

J. S. O. Evans

Department of Chemistry, University Science Laboratories, University of Durham, South Road, Durham DH1 3LE, United Kingdom

(Received 10 July 2000; accepted for publication 13 December 2000)

The effect of pressure on the crystal structure of HfW_2O_8 has been investigated by neutron powder diffraction. At a hydrostatic pressure of 0.62 GPa at room temperature the cubic material transforms, with a 5% reduction in volume, to the same orthorhombic phase that is seen in the isostructural compound ZrW_2O_8 above 0.21 GPa. The transformation is sluggish, requiring about 24 h to complete at constant pressure. Once formed, the orthorhombic phase is retained upon release of pressure. Upon heating to 360 K, the metastable orthorhombic phase transforms back to the cubic phase. The substantially higher pressure for the cubic-to-orthorhombic transition in HfW_2O_8 , compared to ZrW_2O_8 , may be important for the application of this material in composites with controlled thermal expansion because rather large local pressures can occur in such composites.

© 2001 American Institute of Physics. [DOI: 10.1063/1.1347412]

INTRODUCTION

Zirconium and hafnium tungstate, ZrW_2O_8 and HfW_2O_8 , exhibit large isotropic negative thermal expansion over a temperature range from 4 K to above 1000 K.^{1,2} This remarkable behavior makes these materials useful as constituents in composites where an objective is to adjust thermal expansion to a desired value. However, ZrW_2O_8 , which was investigated initially, undergoes a pressure-induced phase transformation at 0.21 GPa with a 5% reduction in volume.^{3,4} The resulting orthorhombic phase is metastable upon release of pressure at room temperature, but converts back to the cubic phase upon heating. Ceramic processing methods and grain interaction stresses in composites can result in local pressures sufficiently large to drive grains of the tungstate through the phase transformation.⁵ If this happens, the composite will exhibit unusual hysteretic thermal expansion behavior as the ZrW_2O_8 grains transform to the orthorhombic phase on cooling, with a 5% reduction in volume, and then transform back to the cubic phase upon heating above 390 K, with a 5% increase in volume.

In this article, we report the results of a study of the effect of applied hydrostatic pressure on the isostructural compound HfW_2O_8 . Hafnium tungstate exhibits the same remarkable negative thermal expansion properties as zirconium tungstate.² However, we show that the pressure-induced phase transformation to the denser orthorhombic phase occurs only at pressures above 0.6 GPa. Thus, this compound may have advantages for use in composites.

SAMPLE PREPARATION AND NEUTRON POWDER DIFFRACTION

A powder sample of HfW_2O_8 was made from $\text{HfOCl}_2 \cdot 6\text{H}_2\text{O}$ and H_2WO_4 used in a 1:2 ratio. The W reactant was dissolved in aqueous ammonium hydroxide. The Hf reactant was dissolved in water and this solution was added to the W solution. This mixture was heated on a hot plate to complete dryness. The resulting solid was then heated in air at 600 °C/h and held at 1200 °C for 2 h and then quickly cooled to room temperature by removing the sample from the furnace.

Neutron powder diffraction data were collected as a function of hydrostatic pressure (0–0.62 GPa) at room temperature and, for the metastable orthorhombic HfW_2O_8 phase following release of pressure, as a function of temperature (50–380 K) at ambient pressure. The experiments were performed on the Special Environment Powder Diffractometer⁶ at the Intense Pulsed Neutron Source, Argonne National Laboratory. Hydrostatic pressure was generated with a helium gas pressure cell. Data versus temperature at ambient pressure were collected using a displacive closed-cycle helium refrigerator with provision for heating above room temperature. Experimental details have been reported elsewhere.⁴

DATA ANALYSIS AND RESULTS

The data were analyzed by the Rietveld method using the GSAS program.⁷ In the pressure cell, as a result of the beam collimation that is an integral part of the cell,⁸ data are collected only at the $\pm 90^\circ$ scattering angles, where the collimation eliminates all Bragg background scattering from the

^{a)} Author to whom correspondence should be addressed; electronic mail: jjorgensen@anl.gov

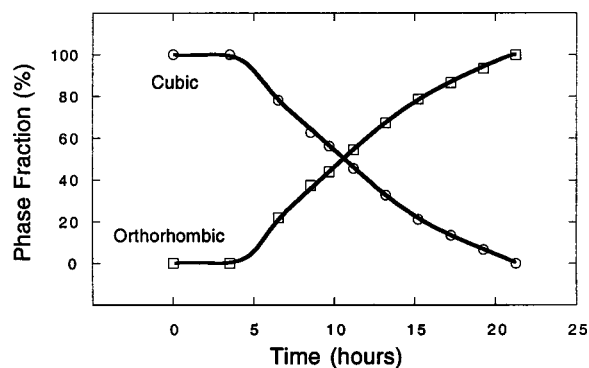


FIG. 1. Phase fractions of the cubic and orthorhombic phases of HfW_2O_8 as a function of time at a constant applied hydrostatic pressure of 0.62 GPa. Error bars are smaller than the points.

cell. In the displax refrigerator and simple radiation furnace used to collect data as a function of temperature, the high resolution back scattering ($\pm 145^\circ$) data are used for the refinements. In both the cubic and orthorhombic phases, the refined parameters included the lattice parameters, atom positions, and isotropic temperature factors. In the orthorhombic phase, temperature factors for the same element (Hf, W, or O) were constrained to be equal to reduce the number of variables.

HfW_2O_8 essentially mimics the behavior of ZrW_2O_8 ^{3,4} except that the pressure-induced cubic-to-orthorhombic phase transformation occurs at a higher pressure and displays sluggish kinetics. The cubic phase remains stable to 0.62 GPa. This is the highest pressure that can be reached in the helium gas pressure cell. At this pressure, the transformation to the orthorhombic phase begins after about 4 h. Figure 1 shows the refined fractions of the cubic and orthorhombic phases as a function of time at constant pressure. The transformation is essentially complete after 24 h. Because the transformation depends on oxygen migration, the sluggish kinetics could be due to the higher transformation pressure (0.62 GPa), as compared to ZrW_2O_8 (0.21 GPa). Oxygen diffusion would be slower at higher pressure as a result of the constriction of the diffusion pathways. Once formed, the orthorhombic phase is metastable and remains after the release of pressure at room temperature. In separate experiments, we investigated whether the cubic-to-orthorhombic transformation would occur at a lower pressure. No evidence for transformation was observed below 0.6 GPa. The experiments included a run in which the pressure was held at 0.52 GPa at room temperature for 11 days with no sign of transformation.

Cell volumes versus pressure for both the cubic and orthorhombic phases are shown in Fig. 2. The data for the cubic phase are taken with increasing pressure, while those for the orthorhombic phase are taken with decreasing pressure after the transformation is complete. The volume compressibilities are compared with those for the two phases of ZrW_2O_8 in Table I. In the cubic phase, HfW_2O_8 has a slightly smaller compressibility than ZrW_2O_8 , but the orthorhombic-phase compressibilities are identical. The slightly smaller volume compressibility for cubic HfW_2O_8 suggests that the transformation to the orthorhombic phase

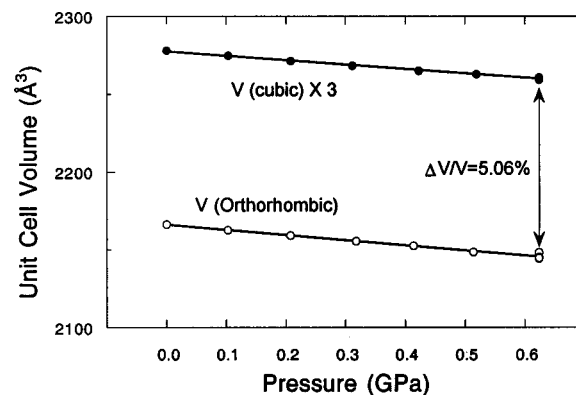


FIG. 2. Unit cell volumes for the cubic and orthorhombic phases of HfW_2O_8 as a function of pressure at room temperature. Data for the cubic phase were taken with increasing pressure. Data for the orthorhombic phase were taken with decreasing pressure after the transformation was complete. Error bars are smaller than the symbols.

might occur at a slightly higher pressure, but is certainly not adequate to explain the threefold increase in transformation pressure observed in experiments. The volume change associated with the transition, 5.06%, is very slightly larger than in ZrW_2O_8 (4.95%). This results simply from the small difference in the compressibilities of the two phases and the higher transformation pressure. At 0.21 GPa, the volume difference for the cubic and metastable orthorhombic phases of HfW_2O_8 is 4.94%, which is identical to the volume change at the transformation in ZrW_2O_8 at 0.21 GPa.

In our previous work on ZrW_2O_8 versus pressure,⁴ we discussed the unusual compression behavior of the cubic phase in an attempt to explain the cause of the transformation. However, because cubic ZrW_2O_8 exists only over a 0–0.21 GPa pressure range, it was difficult to learn the response of individual bond lengths and angles to pressure with the desired precision. The present study on HfW_2O_8 allows some of the key questions to be reexamined. Issues of key importance are the compression of Hf–O and W–O bonds and the pressure-induced changes in the Hf–O–W linking angles. Results from the present study are shown in Fig. 3. Most importantly, the two independent Hf–O–W linking angles both increase with pressure, as was also deduced from the study of ZrW_2O_8 . This counterintuitive behavior is striking evidence of the unusual topology of the MW_2O_8 structure. Whereas most corner-linked framework structures achieve volume reduction under pressure by decreasing the linking angles, because of the topology of the structure, this does not occur for MW_2O_8 . In fact, a distance-least-squares refinement for an idealized cubic

TABLE I. Volume compressibilities $[(\Delta V/\Delta P)/V]$ for the cubic and orthorhombic phases of HfW_2O_8 and ZrW_2O_8 ^a as measured by *in situ* neutron powder diffraction under hydrostatic conditions, using helium gas as the pressure transmitting fluid.

| | HfW_2O_8 (GPa^{-1}) | ZrW_2O_8 (GPa^{-1}) |
|--------------------|--|--|
| Cubic phase | 0.0122(1) | 0.0138(1) |
| Orthorhombic phase | 0.0153(1) | 0.0153(1) |

^aSee Ref. 4.

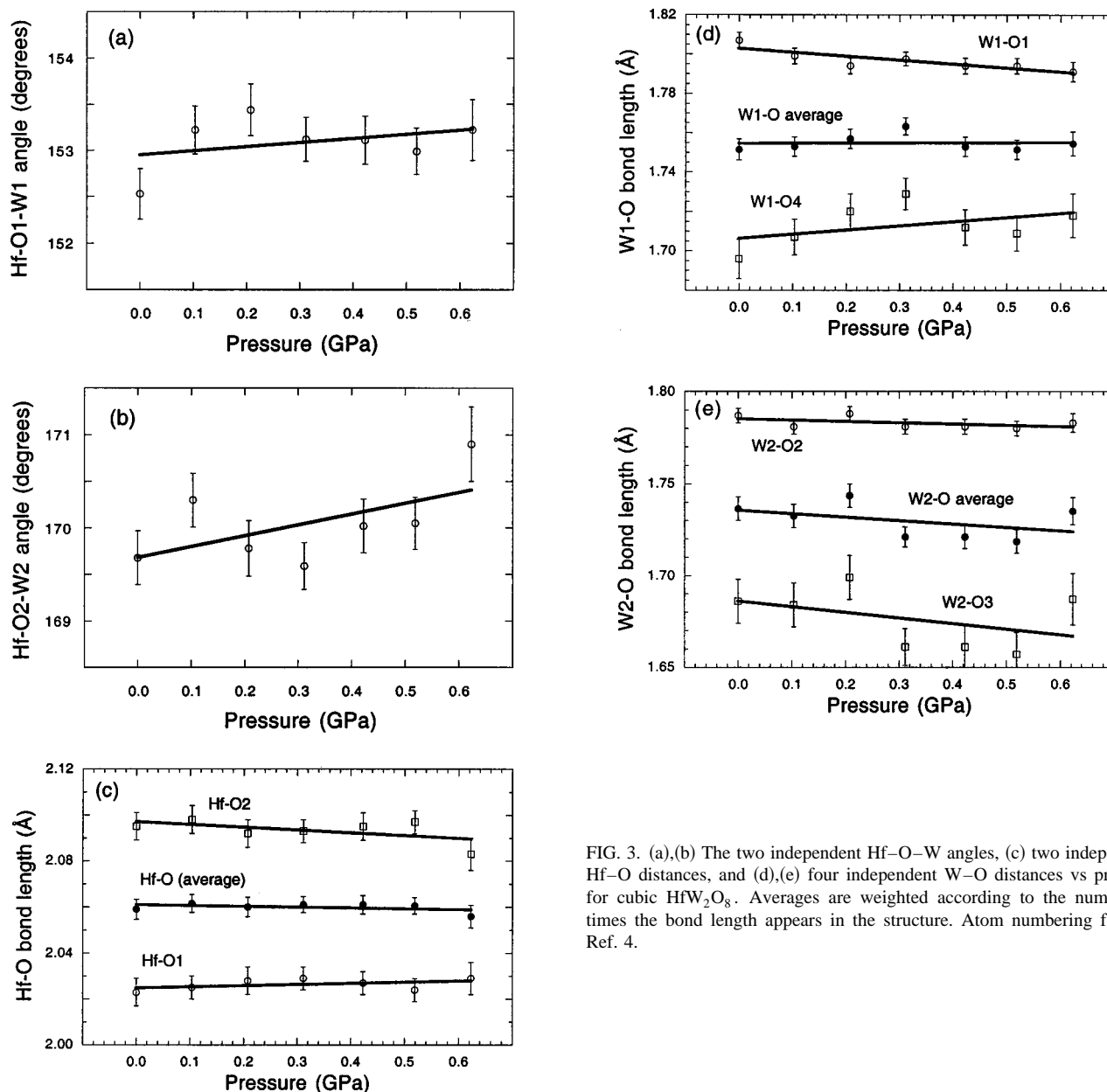


FIG. 3. (a),(b) The two independent Hf–O–W angles, (c) two independent Hf–O distances, and (d),(e) four independent W–O distances vs pressure for cubic HfW_2O_8 . Averages are weighted according to the number of times the bond length appears in the structure. Atom numbering follows Ref. 4.

ZrW_2O_8 structure (with perfect rigid polyhedra) as a function of changing the unit cell volume shows that, over a limited range of cell volumes, compression can occur while the average linking angle increases.⁴ Our experiments confirm the prediction of this model calculation for both ZrW_2O_8 and HfW_2O_8 .

The present data also allow a more accurate determination of the compression of Hf–O and W–O bonds. In the cubic phase, there are two independent Hf–O bond lengths in each HfO_6 octahedron (three of each length) and two independent W–O bonds (three of one length and one of different length) in each of the two independent WO_4 tetrahedra. The behavior of these bond lengths, and the averages for the polyhedra, are shown in Fig. 3. As expected, the average bond compression [expressed as $(\Delta l/\Delta P)/l$] is very small: $-2(2) \times 10^{-3} \text{ GPa}^{-1}$ for Hf–O bonds and $-5(5) \times 10^{-3} \text{ GPa}^{-1}$ for W–O bonds (based on least squares fits of linear functions to the data).

After the orthorhombic phase of HfW_2O_8 is formed at high pressure, it remains stable upon the release of pressure at room temperature. This allows the study of the thermal expansion properties of the orthorhombic phase, as was done for ZrW_2O_8 .^{4,9} The behavior is very similar. At low temperature (below 200 K), the volume thermal expansion of the orthorhombic phase is negative, but it becomes positive above 200 K as the transformation back to the cubic phase is approached (Fig. 4). Taking data at the temperatures shown in Fig. 4 on warming, starting at 50 K, with 3 h data collection times, we found our metastable sample to be orthorhombic at 350 K and cubic at 360 K. The kinetics of this transformation were not investigated; however, work on ZrW_2O_8 ⁹ has shown that there can be kinetic effects, as would be expected for a transformation that depends on thermally activated oxygen migration. The average volume thermal expansion $[(\Delta V/\Delta T)/V]$ of the orthorhombic phase at low temperature (50–100 K) is $-6 \times 10^{-6} \text{ K}^{-1}$. Within the un-

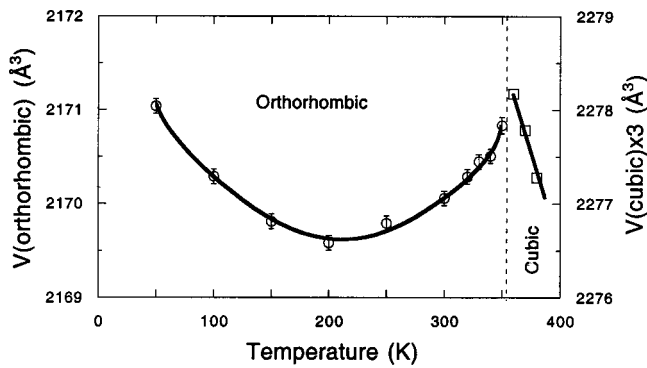


FIG. 4. Unit cell volume upon heating the metastable orthorhombic phase of HfW_2O_8 . At 360 K there is a transformation to the cubic phase. In the cubic phase, error bars are smaller than the symbols.

certainties of the measurement, this is the same as was observed for the metastable orthorhombic phase of ZrW_2O_8 .⁹ Thus, the thermal expansions are the same for both the cubic² and orthorhombic phases of ZrW_2O_8 and HfW_2O_8 .

Above about 200 K, the thermal expansion becomes increasingly positive as the transition back to the cubic phase (at 360 K) is approached (Fig. 4). In a recent article about ZrW_2O_8 ,⁹ we have discussed in detail the basis for this unusual thermal expansion behavior of the orthorhombic phase. At low temperature, the thermal expansion is dominated by phonon contributions and is negative, as for the cubic phases of ZrW_2O_8 and HfW_2O_8 . The magnitude of the negative thermal expansion is considerably smaller because the orthorhombic phase contains additional metal–oxygen bonds that reduce the framework flexibility. This leads to a situation where the negative thermal expansion at the lowest temperature (from phonon modes with negative Gruneisen parameters) is partially compensated at higher temperature as additional phonon modes (with positive Gruneisen parameters) are excited. With increasing temperature, an additional positive contribution to the thermal expansion results from fluctuations in the structure that are made possible by the thermally activated migration of oxygen atoms.

Based on this simple physical picture, we have previously shown⁹ that the linear thermal expansion can be adequately modeled with a function containing three terms: a term to model the low-energy phonon contribution with a negative Gruneisen parameter leading to negative thermal expansion, a second phonon term (associated with higher-energy phonons) with a positive Gruneisen parameter leading to a positive contribution to the thermal expansion at higher temperature, and a thermally activated term describing the contribution of structural fluctuations that are made possible by thermally activated oxygen migration. In this work, the two phonon contributions are described using a simple Einstein model¹⁰

$$\ln\left(\frac{a_{\text{phonon}}}{a_0}\right) = \frac{c_1 \theta_1}{\exp(\theta_1/T) - 1} + \frac{c_2 \theta_2}{\exp(\theta_2/T) - 1}, \quad (1)$$

where a is the lattice parameter, a_0 is the lattice parameter at $T=0$, T is the temperature, θ_1 and θ_2 are characteristic tem-

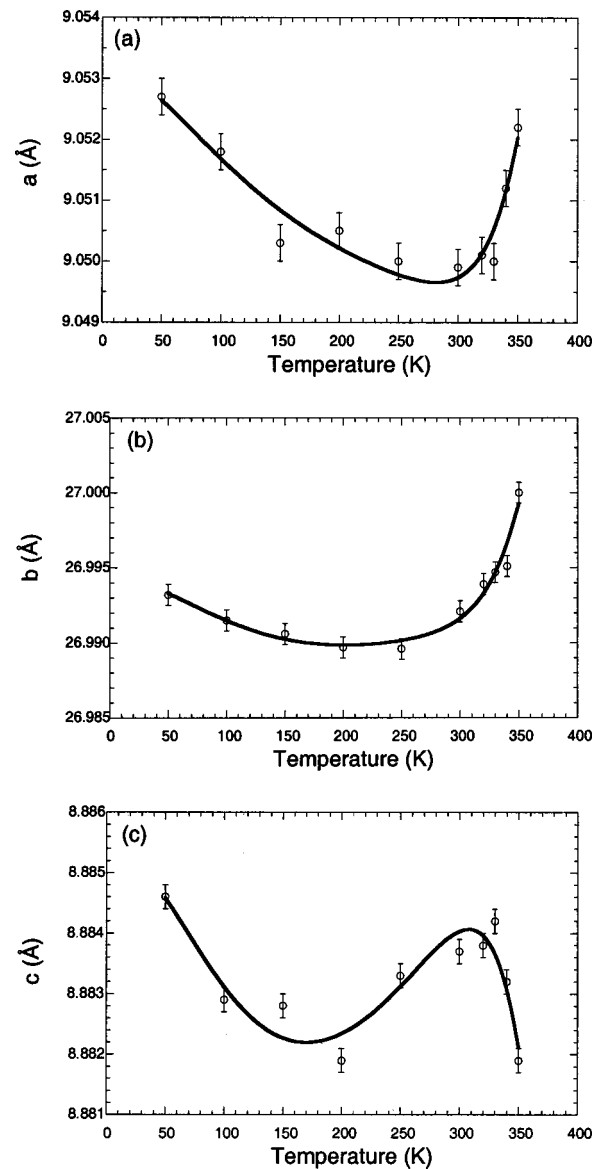


FIG. 5. Unit cell lengths of the metastable orthorhombic phase of HfW_2O_8 as a function of temperature. Data were taken upon heating. Solid lines are a model calculation using the equation $a_{\text{total}}(T) = a_{\text{phonon}}(T) + c_3 \times \exp(-E_A/RT)$, [Eq. (2)], which includes two phonon terms and a thermally activated term.

peratures ($\theta_2 > \theta_1$), and c_1 and c_2 are experimentally determined coefficients for the negative and positive contributions to the thermal expansion, respectively.

A thermally activated term is added to give the expression for the overall thermal expansion

$$a_{\text{total}}(T) = a_{\text{phonon}}(T) + c_3 \exp(-E_A/RT), \quad (2)$$

where E_A is the activation energy for the thermally activated term and c_3 is a coefficient that scales the contribution of this term.

The data for orthorhombic HfW_2O_8 were not taken at low enough temperature and at enough closely spaced temperatures near room temperature to perform a least squares fit where all parameters of this function are varied (as was done for ZrW_2O_8).⁹ However, using the same Einstein temperatures, $\theta_1 = 80$ K and $\theta_2 = 600$ K, and activation energy,

TABLE II. Fixed parameters, θ_1 , θ_2 , E_A , and refined parameters from fitting Eq. (2) to the data for the a , b , and c lattice constants of orthorhombic HfW_2O_8 vs temperature. Numbers in parentheses are standard deviations for the refined parameters. The results of the fittings are shown in Fig. 5

| Parameter | a | $b/3$ | c |
|------------------------------------|-----------|-----------|------------|
| a_0 ($T=0$) (\AA) | 9.0531(4) | 8.9980(4) | 8.8853(5) |
| c_1 (10^{-6} K^{-1}) | -2.4(6) | -1.6(4) | -4.0(8) |
| θ_1 (K) | 80 | 80 | 80 |
| c_2 (10^{-6} K^{-1}) | +2.5(1.5) | +3.1(1.1) | +10.1(1.8) |
| θ_2 (K) | 600 | 600 | 600 |
| c_3 (\AA) | 2600(600) | 2300(500) | -3700(700) |
| E_A (kJ mol^{-1}) | 40 | 40 | 40 |

$E_A = 40 \text{ kJ mol}^{-1}$, as for ZrW_2O_8 and varying only the three coefficients c_i and the $T=0$ values for the lattice parameters, this function provides a good fit to the data for the three orthorhombic axes, as shown in Fig. 5. Values of the coefficients used to fit the model to the data are given in Table II.

CONCLUSIONS

The large difference in the cubic-to-orthorhombic transformation pressure for HfW_2O_8 (0.62 GPa) compared to ZrW_2O_8 (0.21 GPa) is surprising in light of the essentially identical structural chemistry for Hf and Zr in the tungstate compound. Table III shows characteristic bond lengths and angles for the two compounds in the cubic phase. The structure consists of a $\text{Hf}(\text{Zr})\text{O}_6$ octahedron and two symmetry-inequivalent WO_4 tetrahedra that are linked to the $\text{Hf}(\text{Zr})\text{O}_6$ octahedra through shared oxygen atoms. Thus, the $\text{Hf}(\text{Zr})\text{-O}$ distances, W-O distances, and $\text{Hf}(\text{Zr})\text{-O-W}$ linking angles are the most important structural parameters where one might look for a difference between the hafnium and zirconium compounds. As shown in Table III, even with the precision data obtained in these studies, there are no significant

TABLE III. Selected bond lengths and angles in HfW_2O_8 and the corresponding lengths and angles in ZrW_2O_8 .^a These data are the zero-pressure values from a least squares fit of a linear function to the respective length and angle data vs pressure. Numbers in parentheses are standard deviations of the last significant digit.

| Bond length or angle | HfW_2O_8 | ZrW_2O_8 |
|--|--------------------------|--------------------------|
| $\text{Hf}(\text{Zr})\text{-O1}$ (\AA) | 2.045(2) | 2.037(2) |
| $\text{Hf}(\text{Zr})\text{-O2}$ (\AA) | 2.097(3) | 2.100(4) |
| Average $\text{Hf}(\text{Zr})\text{-O}$ (\AA) | 2.071(2) | 2.069(2) |
| W1-O1 (\AA) | 1.803(2) | 1.806(3) |
| W1-O4 (\AA) | 1.706(7) | 1.709(7) |
| Average W1-O (\AA) | 1.779(2) | 1.782(2) |
| W2-O2 (\AA) | 1.785(2) | 1.787(2) |
| W2-O3 (\AA) | 1.686(11) | 1.700(3) |
| Average W2-O (\AA) | 1.760(3) | 1.765(2) |
| $\text{Hf}(\text{Zr})\text{-O1-W1}$ ($^\circ$) | 153.0(2) | 153.4(3) |
| $\text{Hf}(\text{Zr})\text{-O2-W2}$ ($^\circ$) | 169.7(3) | 170.9(2) |

^aData for ZrW_2O_8 and the atom numbering scheme are from Ref. 4.

differences between the two structures. Thus, we have no structural explanation for the large difference in the transformation pressure. This extreme sensitivity of the transformation pressure to subtle differences in chemistry and/or structure is consistent with our previous observation of a small difference in the transformation pressure for two samples of ZrW_2O_8 , for which we were unable to provide an explanation. Such behavior suggests that the transformation properties could also be quite different in nonhydrostatic conditions.

Perhaps more importantly, this work shows that subtle changes in chemical composition can be used to dramatically change the properties of this material under applied pressure. This is particularly important when the tungstate is used as a constituent in a composite where the goal is to achieve a desired overall thermal expansion. In composites, during formation and/or as a function of temperature, the local pressure can easily reach values large enough to cause the transformation of grains of cubic ZrW_2O_8 to the orthorhombic phase. When this transformation occurs, it imparts a strange hysteretic behavior to the composite, as was recently shown in work on composites of ZrW_2O_8 and copper.⁵ Our results reported in this article shows that chemical substitution can be used to overcome this challenge in the application of these remarkable negative thermal expansion tungstate materials. A goal of this article has been to provide the physical parameters for HfW_2O_8 that are needed for use of the material in applications, including the rational design of composites.

ACKNOWLEDGMENTS

The work at Argonne National Laboratory was supported by the U. S. Department of Energy, Office of Science, Contract No. W-31-109-ENG-38. The work at Oregon State University was supported by the National Science Foundation, Grant No. DMR-9308530 and the Oregon Metals Initiative.

- 1 T. A. Mary, J. S. O. Evans, T. Vogt, and A. W. Sleight, *Science* **272**, 90 (1996).
- 2 J. S. O. Evans, T. A. Mary, T. Vogt, M. A. Subramanian, and A. W. Sleight, *Chem. Mater.* **8**, 2809 (1996).
- 3 J. S. O. Evans, Z. Hu, J. D. Jorgensen, D. N. Argyriou, S. Short, and A. W. Sleight, *Science* **275**, 61 (1997).
- 4 J. D. Jorgensen, Z. Hu, S. Teslic, D. N. Argyriou, S. Short, J. S. O. Evans, and A. W. Sleight, *Phys. Rev. B* **59**, 215 (1999).
- 5 C. Verdon and D. C. Dunand, *Scr. Mater.* **36**, 1075 (1997); Holzer, D. C. Dunand, *J. Mater. Res.* **14**, 780 (1999); S. Yilmaz and D. C. Dunand, *J. Mater. Res.* (in press).
- 6 J. D. Jorgensen *et al.*, *J. Appl. Crystallogr.* **22**, 321 (1989).
- 7 A. C. Larsen and R. B. Von Dreele, Los Alamos Internal Report No. 86-748, 1985-1990 (unpublished).
- 8 J. D. Jorgensen, S. Pei, P. Lightfoot, D. G. Hinks, B. W. Veal, B. Dabrowski, A. P. Paulikas, R. Kleb, and I. D. Brown, *Physica C* **171**, 93 (1990).
- 9 J. S. O. Evans, J. D. Jorgensen, S. Short, W. I. F. David, R. M. Ibberson, and A. W. Sleight, *Phys. Rev. B* **60**, 14643 (1999).
- 10 K. Wang and R. R. Reeber, *Appl. Phys. Lett.* **76**, 2203 (2000).